Proc. Natl. Acad. Sci. USA
Vol. 92, pp. 2474–2478, March 1995
Biophysics

Colocalization of calcium entry and exocytotic release sites in adrenal chromaffin cells

(pulsed-laser Ca^{2+} imaging/amperometry/secretion/active zones)

IAIN M. ROBINSON*, JENNIFER M. FINNEGAN†, JONATHAN R. MONCK*, R. MARK WIGHTMAN†, AND JULIO M. FERNANDEZ*

*Department of Physiology and Biophysics, Mayo Clinic, Rochester, MN 55905; and †Department of Chemistry, University of North Carolina, Chapel Hill, NC 27599

Communicated by Royce W. Murray, University of North Carolina, Chapel Hill, NC, December 15, 1994 (received for review September 29, 1994)

ABSTRACT **"Snapshot" images of localized Ca^{2+} influx into patch-clamped chromaffin cells were captured by using a recently developed pulsed-laser imaging system. Transient opening of voltage-sensitive Ca^{2+} channels gave rise to localized elevations of Ca^{2+} that had the appearance of either "hotspots" or partial rings found immediately beneath the plasma membrane. When the Ca^{2+} imaging technique was employed in conjunction with flame-etched carbon-fiber electrodes to spatially map the release sites of catecholamines, it was observed that the sites of Ca^{2+} entry and catecholamine release were colocalized. These results provide functional support for the idea that secretion occurs from "active zone"-like structures in neuroendocrine cells.**

Neurons contain specialized regions at the plasma membrane where secretory vesicles accumulate. These regions, called active zones, were first observed by electron microscopy (1, 2). These active zones are also believed to contain clusters of voltage-sensitive Ca^{2+} channels (3). More recently, localized zones of Ca^{2+} entry, termed hotspots, have been identified in neurons, both on dendrites (4, 5) and at nerve terminals (6), and also in hair cells (7). Furthermore, it has been demonstrated that vesicular secretion is triggered by specific modes of Ca^{2+} influx across the plasma membrane (8–10). This has led to the hypothesis that these sites of Ca^{2+} entry are colocalized at the plasma membrane with sites where vesicles are poised for fusion. Indeed, a standard textbook notion describes just such a scenario for neuronal cells; however, there is no direct functional evidence to support this point. There have been no reports of morphological structures similar to the active zones found in neurons being present in neuroendocrine cells.

A recent report (11) has described the existence of hotspots of localized Ca^{2+} entry in patch-clamped bovine adrenal chromaffin cells following the transient opening of voltage-sensitive Ca^{2+} channels. The pulsed-laser imaging system employed in these studies has an improved spatial and temporal resolution compared with those imaging systems that have previously been used in attempts to capture the early stages of influx of Ca^{2+} into chromaffin cells. The approach adopted is similar to that used in "flash photography," where a brief transient illumination is used to freeze and capture an image. A pulsed laser is used to provide a brief (350 ns), high-intensity (0.25 J) epi-illumination to transiently excite the fluorescent Ca^{2+} indicator dye rhod-2, enabling the capture of "snapshot" images of the intracellular Ca^{2+} concentration. Wightman and colleagues (12) have independently developed carbon-fiber ultramicroelectrodes that are capable of monitoring secretion from areas of 2 μm^2 and have used these fibers to show that catecholamine release occurs from restricted zones in chromaffin cells. In this study we have combined the pulsed-laser imaging system to resolve the intracellular Ca^{2+} distribution and the carbon-fiber microelectrodes to measure, and spatially map, catecholamine release from individual vesicles. We demonstrate here, by combining the two techniques, that the sites of Ca^{2+} entry are indeed colocalized with active zones of catecholamine release in bovine adrenal chromaffin cells. Thus, the spatial and temporal proximity of the trigger for exocytosis—i.e., Ca^{2+} entry—and release are revealed. These results suggest that chromaffin cells contain structures that are functionally akin to the active zones found in neuronal cells.

The publication costs of this article were defrayed in part by page charge payment. This article must therefore be hereby marked "*advertisement*" in accordance with 18 U.S.C. §1734 solely to indicate this fact.

MATERIALS AND METHODS

Cell Preparation and Culture. Chromaffin cells were prepared from bovine adrenal medullae by enzymatic digestion (13). Isolated cells were suspended in Dulbecco's modified Eagle's medium (DMEM) supplemented with 25 mM Hepes, 10% fetal bovine serum, 8 μM 5-fluoro-2′-deoxyuridine, gentamicin at 50 μg/ml, 10 μM cytosine arabinofuranoside, Fungizone at 2.5 μg/ml, penicillin at 25 units/ml, and streptomycin at 25 μg/ml and plated at a density of 100,000 cells per ml on glass coverslips in 35-mm-diameter Petri dishes. Cells were cultured in a humidified atmosphere at 37°C in the presence of 5% CO_2 for 1–5 days prior to use. For experiments, cells were washed in an extracellular medium comprising 120 mM NaCl, 20 mM Hepes, 4 mM $MgCl_2$, 2 mM $CaCl_2$, 0.4% glucose, and 1 μM tetrodotoxin at pH 7.2 (adjusted with NaOH). The patch-pipette solution contained 120 mM cesium D-glutamate, 30 mM Hepes, 8 mM NaCl, 1 mM $MgCl_2$, 2 mM ATP, and 0.3 mM GTP at pH 7.2, with either 100 μM EGTA or, for imaging studies, 0.4 mM rhod-2 (triammonium salt). Experiments were carried out at room temperature.

Measurement of Membrane Capacitance. In some cases we monitored exocytosis by measuring the cell membrane capacitance, using the whole-cell mode of the patch-clamp technique (14), in conjunction with a digital phase detector (15) implemented on a system comprising an IDA data acquisition interface (Indec Systems, Sunnyvale, CA) and an EPC-7 patch-clamp amplifier (List Electronics, Darmstadt, Germany). A sinusoidal voltage (833 Hz, 54 mV peak to peak) on top of a holding potential of −60 mV was applied to the patch-clamped cell, and the current was measured at two different phase angles, ϕ and $\phi - \pi/2$, relative to the stimulus. The phase was periodically adjusted by the phase tracking technique (16), so that the output at ϕ reflected changes in the real part of the cell admittance [Re(ΔY)], whereas the output at $\phi - \pi/2$ reflected changes in the imaginary part of the admittance [Im(ΔY)], which was used as a measure of the cell membrane capacitance (16).

Fluorescence Imaging of Intracellular Ca^{2+} Concentrations. The imaging system consisted of a Zeiss epifluorescence microscope, a Photometrics cooled CCD camera, and a Com-

paq 386 host computer to control image acquisition and image processing with a Mercury array processor. To this was added a high-intensity pulsed coaxial flash lamp dye laser (model LS-1400, Luminex) to provide short (350 ns) high-intensity pulses of illumination and a patch clamp set up with a List EPC-7 patch-clamp amplifier and an Indec IDA15125 interface for data acquisition and synchronization of the laser with the depolarization stimulus. The laser was coupled with a liquid light guide to the epifluorescence port of the microscope and used to illuminate the entire field of view. The lasing dye used was coumarin 521 (0.02 mM in methanol), which gave a suitable emission spectrum for excitation of rhod-2. The epifluorescence filter block contained a 570-nm DRLP dichroic mirror and a 585-nm EFLP emission filter (Omega Optical, Brattleboro, VT). A Zeiss ×40 objective (0.65 n.a.) was used to image the cells. Image pairs were taken for control and depolarizing stimulus pulses (11, 17). The images were filtered for noise reduction (11). The ratio of the stimulus image divided by the control image is displayed as a pseudocolor image representing the fractional change in fluorescence. Since the ratio corrects for differences in indicator concentration, indicator excluded volume, and light path length, the fractional change in fluorescence represents a measure of Ca^{2+} change, provided that the cell does not move between the control and the stimulus image. Previous estimates put the observed Ca^{2+} changes in the region of 200–300 nM, assuming a resting intracellular Ca^{2+} concentration of 100 nM (11).

Amperometric Detection of Catecholamine Secretion. Two types of carbon-fiber electrodes were used to monitor the release of catecholamines: one type was large, having tip diameters similar to those of the cell (≈14 μm), whereas those used to map the release sites had tip diameters of ≈2 μm. In both cases fabrication of the electrodes required the aspiration of a carbon fiber into a capillary pipette, which was then pulled on a micropipette puller. In the case of the larger electrodes (those used for Fig. 1), the carbon fiber was sealed to the glass capillary tube by immersing the tips of the fibers into epoxy. This was cured overnight at room temperature, then at 100°C for 2 hr, and finally at 150°C for a further 2 hr (18). Before use, the tip of the fiber was beveled at 45° with a micropipette beveler, resulting in an elliptically shaped carbon-fiber tip. The carbon electrodes used to spatially map the release of catecholamines (used for Fig. 2) were constructed in a slightly different manner. After the glass pipette was pulled, ≈500 μm of the carbon fiber was exposed beyond the end of the glass capillary tube and was etched in a Bunsen burner flame, resulting in the formation of a carbon cone with a submicrometer tip. The pipettes were then filled with colloidal graphite into which a chromel wire was inserted to establish an electrical connection. The fibers were then insulated with poly(oxyphenylene) (≈1 μm thick) by electrochemical deposition for 8 min at +4 V, and cured for 40 min at 150°C (12, 19, 20). The tip of the fiber was beveled at an angle of 45° with a micropipette beveler for 5 s to remove the insulating layer at the very tip of the electrode. Both types of electrode were held at a voltage of +650 mV, and the redox current was monitored with an Axopatch 1B patch-clamp amplifier; at this voltage, catecholamines are the main substances released from chromaffin granules that will be oxidized.

RESULTS AND DISCUSSION

Amperometry is a powerful technique for monitoring the release of catecholamines from chromaffin cells. Single amperometric "spikes" have been attributed to the release of a single vesicle's contents (21). Fig. 1*a* shows the amperometric recording obtained following brief (50 ms) depolarization to +20 mV of a single patch-clamped adrenal chromaffin cell held at −60 mV. Several spikes (superimposed upon one another) were detected, suggesting that several vesicles fused with the plasma membrane. This view is supported by the simultaneous measurement of cell membrane capacitance which showed a 24-fF step increase after the depolarizing pulse, corresponding to the fusion of 2–24 vesicles (Fig. 1*a*). Randomly occurring single fusion events were often observed; two examples of such events are shown in Fig. 1 *b* and *c*. In both cases each step in membrane capacitance is accompanied by only a single spike, corresponding to the release of the contents of a single vesicle. In Fig. 1*b*, a foot can be seen that precedes the main spike (22, 23); in contrast, there is no observable foot in the event seen in Fig. 1*c*. The simultaneous capacitance measurement shows that the foot developed immediately after fusion began. These results are similar to those reported in mast cells, where the foot was shown to be due to (*i*) the fusion pore that forms between secretory vesicles and the plasma membrane and (*ii*) the manner in which the vesicle's contents are released from a polymer gel matrix that fills the inside of the secretory vesicle (23–25). Similar vesicular association has been inferred in release studies from chromaffin cells (26, 27). The measurements shown in Fig. 1 report only the extent of secretory excursions from the entirety of the plasma mem-

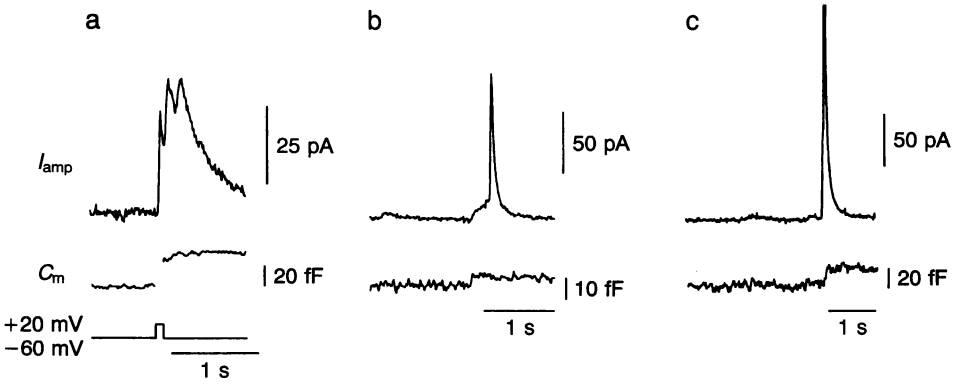

FIG. 1. Secretory events monitored by simultaneous amperometric (I_{amp}) and capacitance (C_m) measurements demonstrate typical patterns of release. *a* shows a wide amperometric response composed of multiple spikes due to the fusion of several secretory vesicles triggered by a 50-ms depolarization to +20 mV from a holding potential of −60 mV. From the magnitude of the capacitance response (24 fF), we estimate that 2–24 vesicles fused with the plasma membrane. The exact number of vesicles that fused is not known, since there is a distribution in their size. The amperometric response shows at least three to five discernible peaks that lag the capacitance step. However, the broad amperometric response (*a*) is likely to be composed of many more spikes. Two particularly large, isolated fusion events are shown in *b* and *c*. A clear lag between the fusion of a vesicle and the main spike of release can sometimes be observed (*b*); however, it is not always present (*c*). This foot contributes to make multiple fusion events, like those of *a*, seem wider than those resulting from single vesicle fusion (compare *a* with *b* and *c*).

brane and provide no spatial data as to where the events took place. To answer this question, we combined pulsed-laser Ca^{2+} imaging with flame-etched carbon-fiber microelectrodes to spatially map the sites of catecholamine release in chromaffin cells.

Fig. 2 *a* and *d* show "snapshot" images of changes in intracellular Ca^{2+} concentration in single patch-clamped bovine adrenal chromaffin cells, obtained with a pulsed-laser imaging system. This imaging technique (11, 17, 28) relies on the transient high-intensity illumination of a pulsed laser (350-ns duration) to excite fluorescent Ca^{2+} indicator molecules (11, 17). Noninactivating Ca^{2+} currents were induced by depolarizing patch-clamped chromaffin cells (in the whole-cell recording mode) from a holding potential of −60 mV to +20 mV for 50 ms. The laser pulse was synchronized to fire 5 ms after the end of the depolarizing pulse. In some instances,

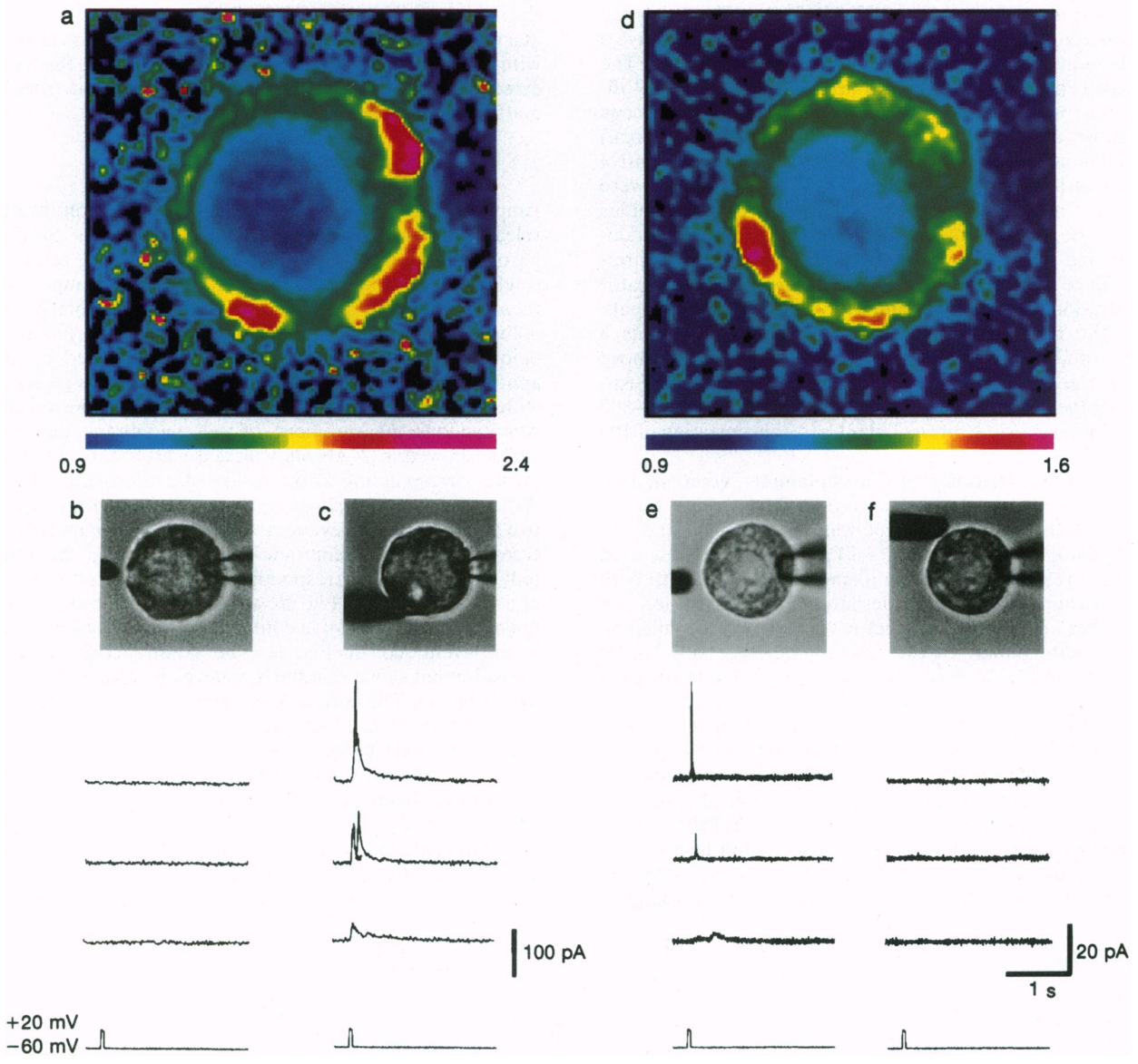

FIG. 2. Ca^{2+} entry and secretion are colocalized in chromaffin cells. Submicrosecond snapshots of intracellular Ca^{2+} distribution reveal local hotspots of elevated Ca^{2+} in response to membrane depolarization. Images are ratios of control (no depolarizing pulse) and stimulus images taken 5 ms after the end of a 50-ms depolarizing pulse to +20 mV from a holding potential of −60 mV; images were taken 5 s apart. The patch pipette is located at the 3 o'clock position in all cases. Discrete influxes of Ca^{2+} lead to the generation of hotspots of Ca^{2+} in some cells (*a* and *d*), whereas in other cells these hotspots are more diffuse and can have the appearance of partial rings (data not shown). Mapping of the catecholamine release sites with flame-etched carbon-fiber microelectrodes revealed that these were colocalized with the areas of Ca^{2+} entry. A pair of brightfield images is shown beneath each of the two Ca^{2+} images; *b* and *c* are of the cell shown in *a*, and *e* and *f* are of the cell shown in *d*. The patch pipette can clearly be seen in the 3 o'clock position in *b, c, e,* and *f*. In both cases the carbon-fiber electrode was initially positioned in the 9 o'clock position (*b* and *e*) (the Ca^{2+} images were obtained with the carbon fibers in this position, where they did not obscure the cell). In the case of the cell in *a–c*, the carbon-fiber electrode was positioned near (1 μm from) the plasma membrane and 6 μm from the nearest Ca^{2+} hotspot (*b*). In this position no amperometric signal was detected (*b*) (3 depolarizing pulses); the carbon-fiber electrode was then moved to 1.5 μm from the hotspot at the 7 o'clock position (*c*) resulting in the detection of an amperometric signal (3 of 3 depolarizing pulses). For the cell depicted in *d–f*, a single Ca^{2+} hotspot at 9 o'clock (*d*) apposed the initial position of the carbon-fiber electrode (*e*) 1.2 μm from the tip of the electrode (the electrode was 0.9 μm from the plasma membrane). Representative amperometric signals recorded from this position are shown immediately beneath the brightfield image (*e*) (in this case 8 of 10 depolarizing pulses gave rise to amperometric spikes). Positioning the fiber at the 11 o'clock position (and virtually touching the plasma membrane), 6.2 μm from the nearest hotspot (*f*) resulted in a decrease in the number of spikes observed (only 2 of 10 pulses stimulated a secretory response). The depolarizing pulse protocol that was used for these experiments is shown at the bottom. (Note: each image is 17 μm^2.)

discrete increases in cytosolic Ca^{2+} levels that had the appearance of hotspots were observed (Fig. 2 *a* and *d*), whereas in other cells these hotspots had merged into partial rings (data not shown). These differences in the patterns of localized Ca^{2+} influx were seen from cell to cell; however, the pattern in each cell was reproducible (11). In all cases the largest increases in intracellular Ca^{2+} concentration were seen immediately beneath the plasma membrane (Fig. 2 *a* and *d*). Depolarizations lasting longer than 100 ms resulted in a loss of the hotspot pattern and a ringlike distribution of Ca^{2+} filling the cytosol beneath the plasma membrane (data not shown). Previous imaging studies using more conventional imaging techniques reported that the effect of depolarizing stimuli on the influx of Ca^{2+} into adrenal chromaffin cells resulted in the elevation of Ca^{2+} as a ring under the plasma membrane (29, 30). The comparatively slow temporal resolution of these systems versus the pulsed-laser imaging system used in this study would account for the fact that hotspots of Ca^{2+} influx have not been described in earlier studies in chromaffin cells. These localized changes in intracellular Ca^{2+} observed during brief ($\leq$50 ms) depolarizations are proposed to represent Ca^{2+} entry through clusters of Ca^{2+} channels in the plasma membrane (11).

Evidence for spatially localized secretion from both cultured (12, 31–33) and *in vivo* (34) chromaffin cells has been reported. Schroeder *et al.* (12) used flame-etched carbon-fiber microelectrodes, which detected the release of catecholamines from areas of only 1–2 μm^2, to demonstrate this point. In these experiments isolated bovine adrenal chromaffin cells were stimulated to secrete with prolonged exposure to either barium, potassium, or nicotine in the presence of extracellular Ca^{2+}. These conditions cause an initial increase in the intracellular Ca^{2+} concentration immediately beneath the plasma membrane. At longer times Ca^{2+} diffuses throughout the cell, resulting in a sustained and homogeneous increase in cytosolic Ca^{2+} (35). Thus the results of Schroeder *et al.* (12) suggest that secretion remains localized in discrete areas of the cell even under conditions which lead to global elevations of Ca^{2+}. Furthermore, experiments with intact chromaffin cells established that elevating intracellular Ca^{2+} by means of various agonists led to appreciable amounts of secretion only in the presence of extracellular Ca^{2+} (21, 35). Recent reports suggested that the pathway of entry and not merely the magnitude of the change in the intracellular Ca^{2+} concentration can determine the extent of the secretory response. It has been shown that opening of different voltage-sensitive Ca^{2+} channels stimulates secretion to different degrees (8–10). These data suggest that there is an important spatial component of the Ca^{2+} signal underlying stimulus–secretion coupling. This raised the interesting question of whether the Ca^{2+} hotspots observed here are colocalized to the zones of secretion described above.

By combining the pulsed-laser imaging technique and the measurement of local catecholamine secretion, we demonstrate that this is indeed the case (see Fig. 2 and Table 1). Fig. 2 shows pseudo-color images of the distribution of intracellular Ca^{2+} for two separate cells following a 50-ms depolarizing stimulus (Fig. 2 *a* and *d*). Brightfield images of the cells depicted in Fig. 2*a* and Fig. 2*d* are shown in Fig. 2 *b* and *c* and Fig. 2 *e* and *f*, respectively. The patch pipette can clearly be seen on the right of the cell, at the 3 o'clock position; in Fig. 2 *b* and *e* the flame-etched fiber can be seen to the left of the cell at 9 o'clock, and in Fig. 2 *c* and *f* it was moved to 7 o'clock and 11 o'clock, respectively. In all cases the carbon-fiber electrodes were placed in close proximity to the plasma membrane [$\approx$0.6 μm (n = 49)] and the distance from the center of the carbon-fiber electrode to the nearest hotspot was measured. Immediately beneath the brightfield images, amperometric recordings are shown that were obtained from the flame-etched electrodes shown in their respective positions above (Fig. 2 *b, c, e,* and *f*). It can be seen that when the fibers were moved to a position adjacent to a Ca^{2+} hotspot, a secretory response was observed (Fig. 2 and Table 1). In contrast, amperometric spikes were observed far less frequently when the fibers were placed in apposition to areas of the cell in which the intracellular Ca^{2+} levels had increased to a lesser extent (Fig. 2 and Table 1). Positioning of the amperometric fiber close to a Ca^{2+} hotspot [1.4 $\pm$ 0.2 μm (n = 38)] resulted in the detection of a secretory response 74% of the times that the cell was stimulated; this figure dropped to only 18% when the fiber was away from any hotspot [3.6 $\pm$ 0.4 μm (n = 19)] (Table 1).

Table 1. Summary of the number of events seen in the amperometric recordings

Electrode position	No. of cells	No. of pulses	No. of spikes	% suecess* rate
Near hotspot	34	216	203	74
Away from hotspot	24	160	33	18

The carbon-fiber electrode was either closely apposed to hotspots [1.4 $\pm$ 0.2 μm (n = 38)] (see Fig. 2) or positioned next to areas in which the intracellular Ca^{2+} levels increased to a lesser extent [3.6 $\pm$ 0.4 μm (n = 19) away from the nearest hotspot]. In all cases the carbon-fiber electrodes were placed in close proximity to the plasma membrane [$\approx$0.6 μm (n = 49)] and the distance to the nearest hotspot was measured from the center of the carbon-fiber electrode. It is clear that positioning the carbon-fiber electrode close to the areas of Ca^{2+} influx resulted in the detection of a secretory response more frequently than when the fiber was away from the Ca^{2+} hotspot.

*A success was defined as the detection of amperometric spikes following stimulation of the cell with a depolarizing pulse. The success rate is thus (no. of successes/total no. of pulses) $\times$ 100. (Note that some depolarizing pulses elicited more than one spike, but for the calculation of the % success rate these mutiple spike events were counted only as single positives.)

The results described above demonstrate that under conditions leading to discrete elevations of Ca^{2+}, secretion occurs from sites that have the functional characteristics of active zones. The next question that needs to be answered is how are these secretory zones organized and what are the roles played by various plasma membrane, vesicular, and cytosolic proteins in establishing these sites in the cell? One scenario that has been envisaged involves the interaction of the vesicle-bound Ca^{2+}-sensing protein synaptotagmin with an integral plasma membrane-bound protein, syntaxin, that has been shown to interact with Ca^{2+} channels (36). Thus targeting of secretory vesicles to specific points on the plasma membrane could result in a clustering of Ca^{2+} channels, or, more simply, that clusters of Ca^{2+} channels could represent the target sites for the docking of secretory vesicles in the first place. Alternatively, cysteine string proteins have been shown to be essential subunits or regulators of presynaptic calcium channels (37), and deletion of this protein in *Drosophila* was shown to inhibit synaptic transmission (38). These proteins were expected to be plasma membrane-associated proteins. Surprisingly, cysteine string proteins are found in the membrane of secretory vesicles of *Torpedo* electric organ (39). These results strongly suggest that a tight association between secretory vesicles and Ca^{2+} channels is required for Ca^{2+} channel function, restricting Ca^{2+} influx to those sites where secretory vesicles are docked in a fusion-ready state (39). Thus, only Ca^{2+} channels associated with docked vesicles would open in response to a depolarizing pulse, providing a possible explanation for the colocalization of Ca^{2+} hotspots and release sites observed in chromaffin cells. The remarkable conservation of the exocytotic machinery (40) suggests that the organization of the catecholamine release sites revealed in this work may be directly applicable to understanding the molecular basis for the organization of the active zones in neurons.

This work was funded by grants from the National Institutes of Health to J. M. Fernandez and the Office of Naval Research to

R.M.W. J. M. Finnegan was supported by a Department of Education predoctoral fellowship.

1. Couteaux, R. & Pécot-Dechavassine, M. (1970) *C. R. Seances Acad. Sci. Sér.* **D271,** 2346–2349.
2. Heuser, J. E. (1989) *Q. J. Exp. Physiol.* **74,** 1051–1069.
3. Pumplin, D. W., Reese, T. S. & Llinás, R. (1981) *Proc. Natl. Acad. Sci. USA* **78,** 7210–7213.
4. Muller, W. & Connor, J. A. (1991) *Nature (London)* **354,** 73–76.
5. Guthrie, P. B., Segal, M. & Kater, S. B. (1991) *Nature (London)* **354,** 76–80.
6. Llinás, R., Sugimori, M. & Silver, R. B. (1992) *Science* **256,** 677–679.
7. Issa, N. P. & Hudspeth, A. J. (1994) *Proc. Natl. Acad. Sci. USA* **91,** 7578–7582.
8. Hirning, L. D., Fox, A. P., McCleskey, E. W., Olivera, B. M., Thayer, S. A., Miller, R. J. & Tsien, R. W. (1988) *Science* **239,** 57–61.
9. Wheeler, D. B., Randall, A. & Tsien, R. W. (1994) *Science* **264,** 107–111.
10. Artalejo, C. R., Adams, M. E. & Fox, A. P. (1994) *Nature (London)* **367,** 72–76.
11. Monck, J. R., Robinson, I. M., Escobar, A., Vergara, J. & Fernandez, J. M. (1994) *Biophys. J.* **67,** 505–514.
12. Schroeder, T. J., Jankowski, J. A., Senyshyn, J., Holz, R. W. & Wightman, R. M. (1994) *J. Biol. Chem.* **269,** 17215–17220.
13. Burgoyne, R. D., Morgan, A. & O'Sullivan, A. J. (1988) *FEBS Lett.* **238,** 151–155.
14. Neher, E. & Marty, A. (1982) *Proc. Natl. Acad. Sci. USA* **79,** 6712–6716.
15. Joshi, C. & Fernandez, J. M. (1988) *Biophys. J.* **53,** 885–892.
16. Fidler, N. & Fernandez, J. M. (1989) *Biophys. J.* **56,** 1153–1162.
17. Monck, J., Escobar, A., Robinson, I., Vergara, J. & Fernandez, J. (1994) *Biophys. J.* **61,** A351 (abstr.).
18. Kawagoe, K. T., Zimmerman, J. B. & Wightman, R. M. (1993) *J. Neurosci. Methods* **48,** 225–240.
19. Kawagoe, K. T., Jankowski, J. A. & Wightman, R. M. (1991) *Anal. Chem.* **63,** 1589–1594.
20. Strein, T. G. & Ewing, A. G. (1992) *Anal. Chem.* **64,** 1368–1373.
21. Wightman, R. M., Jankowski, J. A., Kennedy, R. T., Kawagoe, K. T., Schroder, T. J., Leszczyszyn, D. J., Near, J. A., Diliberto, E. J., Jr., & Viveros, O. H. (1991) *Proc. Natl. Acad. Sci. USA* **88,** 10754–10758.
22. Chow, R. H. & Neher, E. (1992) *Nature (London)* **356,** 60–63.
23. de Toledo, G. A., Fernandez-Chacon, R. & Fernandez, J. M. (1993) *Nature (London)* **363,** 554–557.
24. Monck, J. R. & Fernandez, J. M. (1994) *Neuron* **12,** 707–712.
25. Robinson, I. M. & Fernandez, J. M. (1994) *Curr. Opin. Neurobiol.* **4,** 330–336.
26. Jankowski, J. A., Schroeder, T. J., Ciolkowski, E. L. & Wightman, R. M. (1993) *J. Biol. Chem.* **268,** 14694–14700.
27. Jankowski, J. A., Finnegan, J. M. & Wightman, R. M. (1994) *J. Neurochem.* **63,** 1739–1747.
28. Kinosita, K., Jr., Ashikawa, I., Hibino, M., Shigemori, M., Yoshimura, H., Itoh, H., Nagayama, K. & Ikegami, A. (1988) *Proc. SPIE Int. Soc. Opt. Eng.* **909,** 271–277.
29. Cheek, T. R., O'Sullivan, A. J., Moreton, R. B., Berridge, M. J. & Burgoyne, R. D. (1989) *FEBS Lett.* **247,** 429–434.
30. Neher, E. & Augustine, G. J. (1992) *J. Physiol. (London)* **450,** 273–301.
31. Phillips, J. H., Burridge, K., Wilson, S. P. & Kirshner, N. (1983) *J. Cell Biol.* **97,** 1906–1917.
32. Hesketh, J. E., Ciesielski-Treska, J. & Aunis, D. (1981) *Cell Tissue Res.* **218,** 331–343.
33. Cheek, T. R., Jackson, T. R., O'Sullivan, J. A., Moreton, R. B., Berridge, M. J. & Burgoyne, R. D. (1989) *J. Cell Biol.* **109,** 1219–1227.
34. Carmichael, S. W., Brooks, J. C., Malhotra, R. K., Wakade, T. E. & Wakade, A. R. (1989) *J. Electron Microsc. Tech.* **12,** 316–322.
35. Burgoyne, R. D. (1991) *Biochim. Biophys. Acta* **1071,** 174–202.
36. Bennet, M. K., Calakos, N. & Scheller, R. H. (1992) *Science* **257,** 255–259.
37. Gundersen, C. B. & Umbach, J. A. (1992) *Neuron* **9,** 527–537.
38. Mastrogiacomo, A., Parsons, S. M., Zampighi, G. A., Jenden, D. J., Umbach, J. A. & Gundersen, C. B. (1994) *Science* **263,** 981–982.
39. Zinsmaier, K. E., Eberle, K. K., Buchner, E., Walter, N. & Benzer, S. (1994) *Science* **263,** 977–980.
40. Bennet, M. K. & Scheller, R. H. (1993) *Proc. Natl. Acad. Sci. USA* **90,** 2559–2563.